Welding in the World (2019) 63:43–51
https://doi.org/10.1007/s40194-018-0650-2

RESEARCH PAPER

Formation of multi-axial welding stresses due to material behaviour during fabrication of high-strength steel components

Dirk Schroepfer[1] · Arne Kromm[1] · Thomas Kannengiesser[1]

Received: 16 August 2017 / Accepted: 11 September 2018 / Published online: 26 September 2018

Abstract

Today, an expanding application of high-strength steels in modern welded constructions can be observed. The economical use of these steel grades largely depends on the strength and reliability of the weldments. Therefore, the special microstructure and mechanical properties of these grades have to be taken into account by keener working ranges regarding the welding parameters. However, performance and safety of welded components are strongly affected by the stresses occurring during and after welding fabrication locally in the weld seam and globally in the whole component, especially if the shrinkage and distortion due to welding are restrained. Some extensive studies describe the optimization of the welding stresses and the metallurgical effects regarding an adapted welding heat control. Lower working temperatures revealed to be particularly effective to reduce the local and global welding-induced residual stresses of the complete weld significantly. However, decreased interpass temperatures cause concurrently higher stresses during welding fabrication. This work shows strategies to reduce these in-process stresses. With help of multi-axial welding stress analyses in component-related weld tests, using a special 2-MN-testing facility, differences in stress build-up are described in detail for root welds, filler layers and subsequent cooling to ambient temperature.

Keywords Residual stresses · GMA welding · Restraint · High-strength steels · Process parameters

1 Introduction

For economic and ecological reasons, high-strength fine-grained structural steels are applied increasingly in modern steel construction, such as mobile cranes [1]. Without those steel grades, today's extends of booms and load-bearing capacities of this cranes, e.g. necessary for the assembly of wind power stations, are virtually impossible. With respect to the welds in high-strength steel components, information about residual stress levels and distributions due to welding is needed to ensure ideal performance of the load-bearing capacity and safety at once. This is basically reduced to the high yield-to-tensile ratio of these grades. High tensile residual stresses—especially in case of multi-axial stressing—compromise the cracking resistance and might provoke premature failure in service [2]. However, on the other hand, an across-the-board assumption of such high stresses throughout the proof of load-bearing capacity—according to current standards [3]—results in highly conservative designs, which are in contradiction to lightweight construction and do not allow an economical use of high-strength steel grades.

Moreover, during and after fabrication of component welds, external restraints of the surrounding area and circumjacent structures among the local restraints of the weld seam possess an extensive influence on the welding stresses; see Fig. 1. The restraint is subjected to the design of the welded structure. Hence, the influence on the welding stresses should be accounted to near and far field effects. Without an external restraint, a free shrinkage transverse to the weld Δy and a free angular distortion $\Delta\beta$ is allowed and restraint stresses σ_{rs} form while welding and cooling due to inhomogeneous volume changes locally in the weld area and HAZ [6]. If the lateral distortion Δy is globally restrained, normal reaction stresses σ_y occur, which superimpose the near field restraint stresses. In general, in component welds also, the angular distortion $\Delta\beta$ is restrained, which causes bending moments M_x and stresses σ_{Mx} while welding and cooling. Regarding

Recommended for publication by Commission II - Arc Welding and Filler Metals

✉ Dirk Schroepfer
dirk.schroepfer@bam.de

[1] Bundesanstalt für Materialforschung und-prüfung (BAM), Unter den Eichen 87, 12205 Berlin, Germany

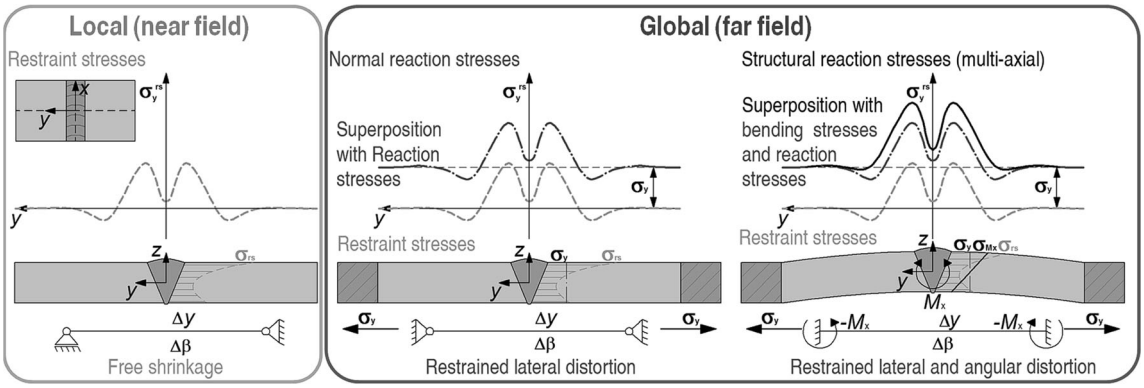

Fig. 1 Schematic of classification and superposition of welding induced stresses dependent on restraint condition according to [4, 5]

the formation of multi-axial welding stresses, these global bending stresses are additionally superimposed to the local restraint stresses. For that, for any detailed investigations of the stress build-up, welding experiments should consider realistic conditions of restraints as well as thermal conduction in the welds, according to several recent works [7, 8]. Satoh [8] established the restraint intensity concepts. With that, the restraint transverse R_{Fy} to the weld and the bending restraint around the weld seam axis R_{Mx} can be quantified. In this context, several works addressed to the influence and interaction of base and filler material grade and heat control [9–12] already; see Fig. 2. In those analyses, primarily for root welding, severe welding stresses were found, since the load-bearing cross section is still relatively small in comparison to the occurring forces and stresses. It was observed that already during fabrication, the welding loads and stresses—according to their scope—indicate remarkable interactions with the main influence factors; see Fig. 2. Hence, the focus of this work is the in situ detection of forces and moments in relation to the weld seam build-up by means of welding experiments in a special in-house developed testing facility at BAM. This work was conducted in the scope of two AiF-research projects [13, 14].

2 Experimental

V-Butt joints were welded by an automated multilayer GMAW process under free shrinkage and in special testing facilities, like the 2-MN-testing facility, which allowed a defined restraint as well as an in situ analysis of the reaction forces and moments simultaneously, while welding and cooling; see Fig. 3. With a specific variation of parameters by means of DoE for an adequate statistical evaluation of the results, the effects and interactions of base and filler material grade and heat control on the welding stress build-up in high-strength steels could be analysed for certain defined restraint conditions; see Table 1. Also, the effect of the formation of the root weld was examined using slender seam preparations associated with a modified spray arc process. High-strength fine-grained structural steels S690QL and S960QL were welded with matching high-strength solid wire; see Table 2.

To monitor the working temperatures, thermocouples were attached 10 mm adjacent to the weld. $\Delta t_{8/5}$-cooling times were determined by a two-colour pyrometer (range 350 to 1300 °C) at the weld layer surface. The influence factors according to Fig. 2 were varied: heat control, welding parameters and seam configuration as well as the restraint intensity

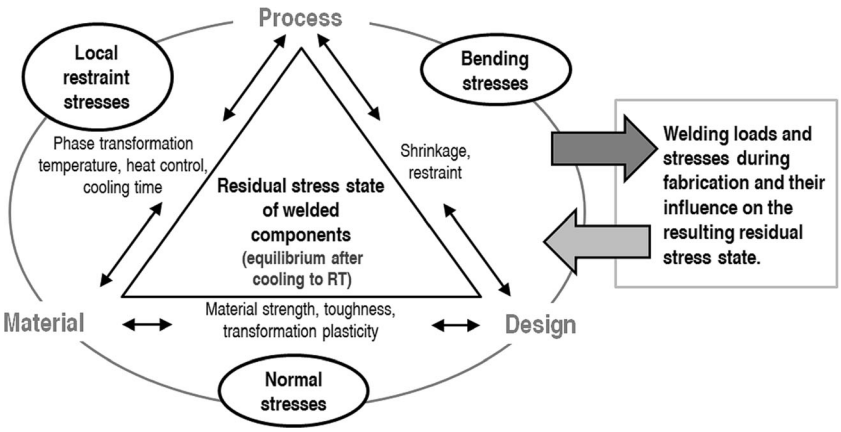

Fig. 2 Influences on welding stresses during and after fabrication according to [15]

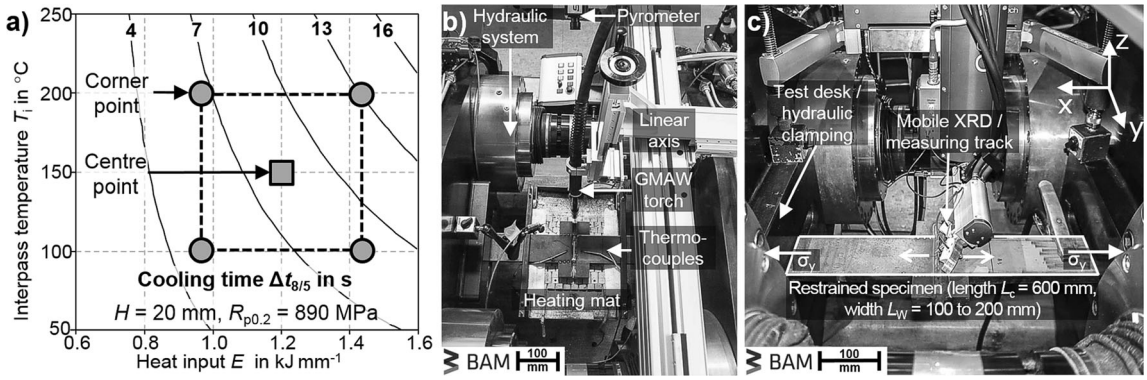

Fig. 3 **a** Variation of heat control using design of experiments (DoE, Example: S960QL, 20 mm plate thickness) over a contour plot of the statistical evaluation of the determined $\Delta t_{8/5}$-cooling times; overview of **b** weld test setup in the 2-MN-testing facility and **c** residual stress analysis in the testing facility at a clamped specimen [4]

for two different high-strength steel grades in 8-mm- and 20-mm-thick plates; see Table 1. Modified welding parameters enabled the welding of 30° V-groove joints with a less amount of weld runs. High-strength quenched and tempered fine-grained structural steels S690QL and S960QL were welded with matching high-strength solid filler wire; see Table 2. Centre point tests were repeated to provide an adequate statistical basis for the results. The heat control range was selected according to $\Delta t_{8/5}$-cooling time ranges specified by steel producers; compare Fig. 3a. For local stress analyses in the weld seam area, mobile X-ray diffraction (XRD) was used for the unrestrained and the restrained specimens in the testing facilities; see Fig. 3c.

3 Main effects on global stresses

As described in references [4, 5, 16, 17], the restrained angular and lateral distortions cause global reaction forces and moments, which were measured using the 2-MN-testing facility; see Fig. 4. In this welding experiments, for the first time, the reaction moments $M_x(t)$ based on the neutral axis of the actual load bearing height of the weld were analysed via a compensation calculation (compare Fig. 4a, b) while welding and cooling [4]. In Eq. 1, the simplified compensation calculation is given according to Fig. 4b.

$$M_x(t) = F_{y,up}(t)a_{y,up}(t) - F_{y,low}(t)a_{y,low}(t) + K\left(F_{y,left}(t)\right) \quad (1)$$

Therefore, the height of the neutral axes of the specimen in the testing facility $H_{NA,P}$ and of the actual load bearing cross section of the welded specimen $H_{NA,N}$ in relation to the centre lines of the testing facilities piston rods were considered. The factor K compensates influences of additional reaction moments occurring due to $F_{y,left}(t)$. With help of the measurement of the forces ($F_{y,up}(t)$, $F_{y,low}(t)$ and $F_{y,left}(t)$) using load cells at each piston rod, the resulting total reaction forces F_y and moments M_x of the welded specimen were analysed; see Fig. 4c [4, 5].

In the shown example, the graphs of the reaction force and reaction moment are qualitatively equal, since the reaction

Table 1 Welding parameters; variation of design, process and material by means of DoE [4, 13, 14]

Seam geometry	Welding current	Welding voltage	Welding speed	Feeding speed	Welding process
V-type, 45°	220 to 290 A	22 to 29 V	280 to 550 mm/min	6.0 to 8.7 m/min	Conv.*
V-type, 30°	320 A	29 V	400 to 420 mm/min	11 m/min	Mod.*
Varied design parameters	Varied heat control and welding process		Varied material, BM/FM		
Groove angle [°]: 30 and 45	Working temperature $T_{p/i}$ [°C]: 50 to 200		S690QL/G69[b]		
Plate thickness [mm]: 8 and 20	Heat input [kJ/mm]: 0.6 to 1.6		S960QL/G89[c]		
Restraint intensity [kN/(mm·mm)]: 0[a] to 4 [b]	Welding process*: Conv./Mod.		S960QL/G89, root G46 [d]		

* Welding process of the power source: Conv.: transitional arc, Mod.: modified spray arc

[a] Free shrinking;

[b] EN ISO 16834-A-G 69 6 M21 Mn4Ni1.5CrMo

[c] EN ISO 16834-A-G 89 6 M21 Mn4Ni2CrMo

[d] EN ISO 14341-A-G 46 4M21 4Si1

Table 2 Chemical composition (FES, Fe balanced) and mechanical properties of the 20-mm-thick test materials [4, 13, 14]

Element in %	C	Si	Mn	Cr	Mo	Ni	V	Nb	Ti
Base material (S690QL, EN 10025-6)	0.14	0.32	1.15	0.30	0.17	0.07	0.009	0.005	0.010
Base material (S960QL, EN 10025-6)	0.12	0.22	1.24	0.20	0.61	0.05	0.040	0.015	0.003
Property	$R_{p0.2}$ in MPa	R_m in MPa		A_5 in %		Av in J at − 40 °C		HV10	
S690QL	768	821		19		198		270	
S960QL	1035	1050		17		96		332	

force above the neutral axis of the weld $F_{y,up}$ is ever greater than below the neutral axis $F_{y,low}$ during welding and cooling to ambient temperature. According to the systematic parameter variation within the analyses, these studies [4, 5, 16, 17] revealed—consistently to other recent works [18–21]—that the heat control has a major influence on the global forces and moments in the weld. Figure 5a shows the build-up of the reaction moment for two similar welds with S690QL for different interpass temperatures $T_i = 100$ °C and 200 °C.

It was observed that the first weld runs, especially the root weld, cause significantly higher stresses while cooling to a lower interpass temperature, although lower interpass temperatures are beneficial for a considerable reduction of the reaction moments after completion of the weld and cooling to ambient temperature. This implies that the weld metal is sufficiently ductile and the inhomogeneous transversal shrinkage forces over plate thickness direction of the first weld runs could be systematically reduced due to the ability of plasticisation during cooling and relaxation during the next weld run and heat input. As long as these inhomogeneous reaction forces are effectively reduced by the heat input of the following weld sequence, lower working temperatures may cause a comparatively low build-up of the end reaction moment. Positive bending moments cause bending stresses at the top side of the weld after cooling to ambient temperature. The superposition of these bending stresses and the normal reaction stresses results in total reaction stresses at the top side of the weld [4, 5, 16, 17]. Figure 5b shows an effect diagram of the mean values of the reaction moment and total reaction stresses at specimen top side as a function of the interpass temperature after statistical evaluation of all weld tests in the 2-MN-testing facility. Furthermore, the contour plot of the total reaction stress vs. interpass temperature and bending restraint intensity in Fig. 6a reveals that especially at high restraint conditions with high bending restraints, lower working temperatures are exceedingly beneficial for an effective welding stress reduction. However, at the same time, the low interpass temperatures produce a significant elevation of the welding stresses particularly for the root welds; see Fig. 6b. In order to prevent crack initiation and damages while welding

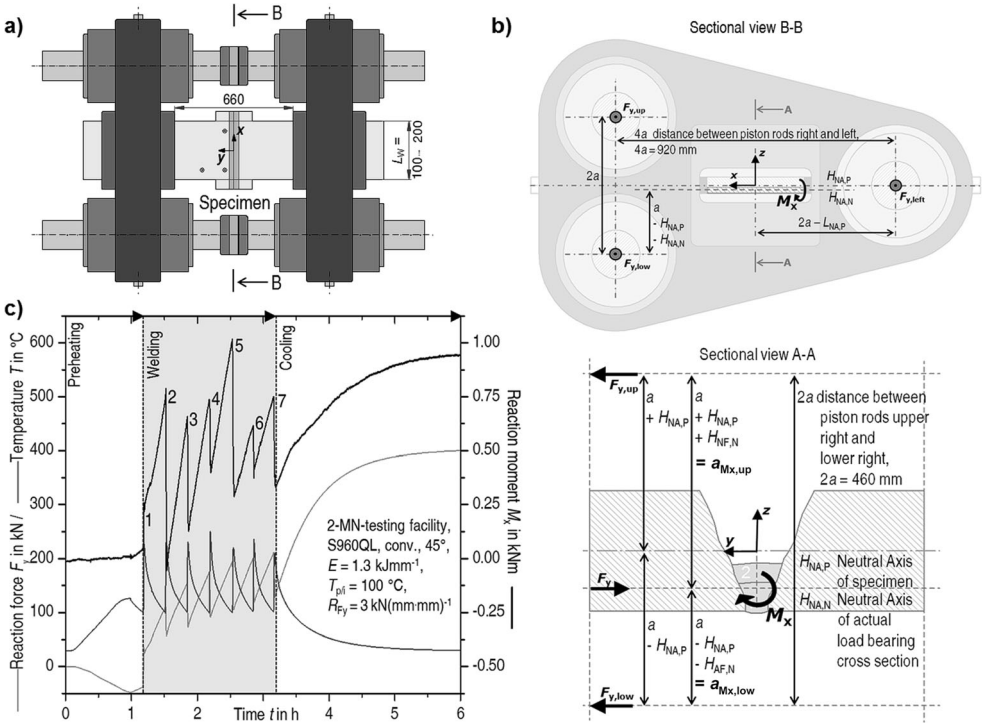

Fig. 4 Schematic of the 2-MN-testing facility (**a**) and compensation calculation for reaction moments based on the neutral axis of the actual load bearing weld cross section (**b**), **c** temperature $T(t)$, reaction forces $R_{Fy}(t)$ and moments $M_x(t)$ during a weld test in the 2-MN-testing facility [4]

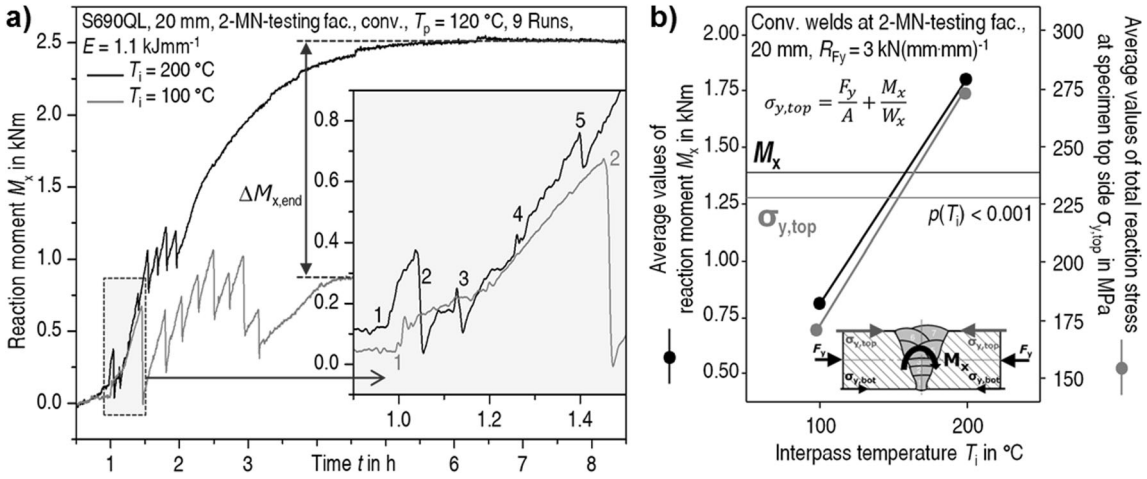

Fig. 5 **a** Reaction moments $M_x(t)$ for two weld tests with different interpass temperatures with detail for the first welding sequences; **b** statistical evaluation of all weld tests with conventional welding process in the 2-MN-testing facility at R_{Fy} = 3 kN(mm mm)$^{-1}$, mean values of the reaction moment M_x and total reaction stress at specimen top side $\sigma_{y,top}$ vs. interpass temperature T_i [4]

fabrication, adapted procedures should be found to reduce these welding stresses.

4 Stress reduction during fabrication

In reference [17], a narrow weld groove in combination with the modified spray arc was used to optimise the welding-induced stresses. In the study, it revealed that the fewer number of weld runs and less eccentricity of the narrow weld groove results in significantly reduced total reaction stresses after cooling to ambient temperature, see Fig. 7.

It was shown as well that the narrow groove leads to an increased height of the root weld, which involves a higher load bearing cross section. Although the reaction stresses while welding are similar for both root welds (see Fig. 7b) and the reaction forces are higher for the modified weld while cooling (see Fig. 7a), significantly reduced reaction stresses due to the increased cross section revealed at interpass temperature (see Fig. 7c). With the analysis of the reaction moment based on the actual neutral axis of the load bearing section, also the build-up of the maximum bending stresses had been investigated. Therefore, Fig. 8 shows the superposition of the normal reaction stresses and of the maximum bending stresses forming at the top side of the actual weld cross section.

It is obvious that the higher reaction stresses and moments occurring in the broader weld groove are additionally detrimental regarding the welding stress increase at the weld top side because of the lower section modulus of the smaller cross section. In contrast to the root weld at the narrow weld groove, the maximum total reaction stresses at the top side of the root $\sigma_{y,topW}$ of the conventional weld are limited due to the yield strength at temperature of the predominating martensitic microstructure of the root weld at interpass temperature T_i = 100 °C; see. Fig. 8. Hence, the experiments showed that especially at high restraints and bending restraints, low narrow groove welds are greatly beneficial for welding stress reduction during fabrication, particularly for materials with low susceptibility to hot cracking.

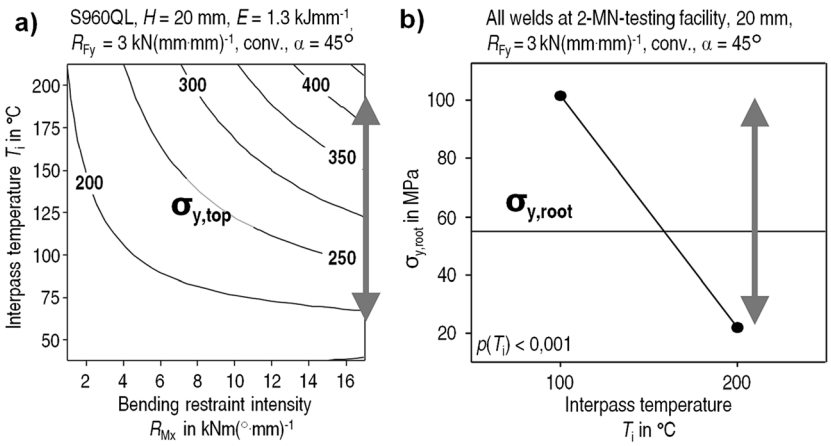

Fig. 6 Statistical evaluation: **a** contour plot of the total reaction stresses at the top side of the specimens $\sigma_{y,top}$ at given hold point vs. interpass temperature T_i and bending restraint intensity R_{Mx}, **b** effect diagram of the mean values of normal reaction stresses of the root weld after cooling to interpass temperature as a function of the interpass temperature T_i for all conventional weld tests in the 2-MN-testing facility at R_{Fy} = 3 kN(mm mm)$^{-1}$ [4]

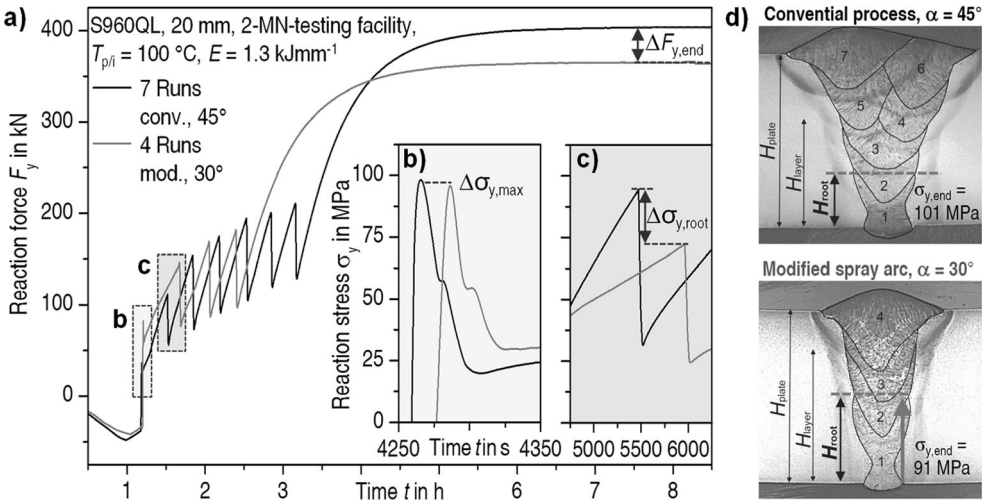

Fig. 7 **a** Reaction force $F_y(t)$ for two weld tests with different seam geometry and welding process, details of reaction stress $\sigma_y(t)$ for welding (**b**) and cooling (**c**) of the root, **d** cross sections of the two different welds [4, 17]

If the welding stresses during fabrication cannot be reduced by a narrow welding groove, in general, ductile filler metals are applied for root welding of thick walled higher-strength steel structures. It is well-known that an undermatching filler material is beneficial for welding stress reduction. However, the effect on the global welding stresses was never quantified in component-related analyses. And the application of more ductile filler metal is limited, since an excessive percentage of the load bearing cross section would drop the strength of the weld seam below the strength requirements. Therefore, Fig. 9 shows the reaction moment of two similar weld tests in the 2-MN-testing facility with S960QL. In one of these welds instead of the matching G89 filler material, the undermatching G46 (mismatch factor approx. 0.5) was applied. Although the comparison of the bending moments $M_x(t)$ shows qualitative equal graphs, it is also obvious that the bending moment of the weld with the ductile filler metal for the root is approx. ΔM_x = 0.25 kNm lower. A detailed analysis reveals that the application of less strength filler materials for root welding results in significantly reduced stresses while welding and cooling of the root layer. The multiaxial examination of the total reaction stresses at the top side of the root weld $\sigma_{y,topW}(t)$ (compare Fig. 8) is presented for root welding and cooling to interpass temperature. The total reaction stresses during cooling do not exceed the yield strength at temperature of the predominating microstructure in the root weld. Hence, the maximum reaction stresses at of the root are approx. $\sigma_{y,topW}$ = 300 MPa for the ductile and approx. $\sigma_{y,topW}$ = 700 MPa for the matching high-strength root weld. Although these reaction stresses are obviously relieved transiently due to the heat input of the subsequent first filler bead, the reaction moment and stresses remain lower in the weld with the undermatching root until the completion of the weld and subsequent cooling to ambient temperature. The higher transformation temperature and higher strain

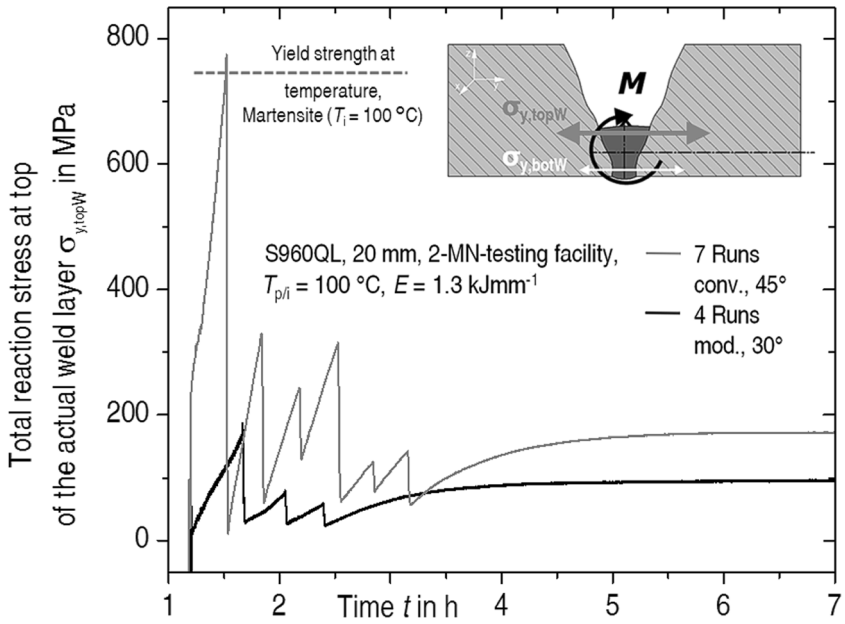

Fig. 8 Reaction stress at the top side of the actual weld layer force $\sigma_{y,topW}(t)$ for two weld tests with different seam geometry and welding process [4, 17]

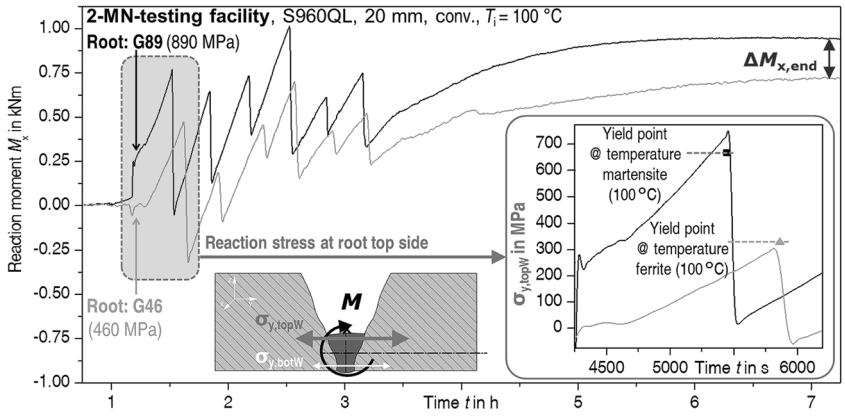

Fig. 9 Reaction moment $M_x(t)$ of a restrained weld in the 2-MN-testing facility (restraint intensity $R_{Fy} = 3$ kN(mm mm)$^{-1}$, with S960QL, plate thickness 20 mm) for two different grades of filler materials for root welding; detail reaction stresses at the top side of the root weld while cooling [4]

capability of the lower strength filler materials have, therefore, beneficial effects on the root stress, but especially on the bending moment build-up, which is significantly reduced.

However, it should be taken into account that undermatching root welds may lessen the strength and, hence, the performance of high-strength component welds in service. Furthermore, high-strength weld metals in filler beads may have beneficial effects on the final stress build-up [22]. The multi-axial analyses of the reaction forces finally allowed the comparison of the bending moment build-up of welds with a different strength of the filler material; see Fig. 10. It is obvious that the scattering between two similar weld tests is way smaller than the variation of the reaction moment build-up between the two weld tests with different materials.

Due to the application of a ductile filler material G46 for root welding of the S960QL already, a lower bending moment is obvious after cooling to interpass temperature $T_i = 150$ °C (see also Fig. 9) compared to the filler material G69, applied for the S690QL. Furthermore, it reveals for the first filler bead that the transient relief of the bending moment is larger for the higher strength filler material G89 and that the transition and slope of the transient increase of the bending moment while cooling to interpass temperature is smaller compared to the lower strength filler material G69. According to reference [22], this is due to the lower phase transformation temperature of the higher strength filler material, which produces higher compressive forces due to the restrained volume expansion. In addition, the predominant displacive transformation in martensitic microstructure has a higher shear component of approx. 24% compared to the phase transformation in ferritic or bainitic microstructures, which leads to a more effective compensation of tensile reaction forces and stresses [23]. Since these effects appear in each weld sequence of the filler beads, after cooling to ambient temperature, the mean values of the reaction moments and total reaction stresses at the weld top side are significantly lower for the S960QL-welds by approx. 30% and 25%, respectively, compared to the S690QL-welds.

5 Consequences

The local residual stresses in the weld, HAZ and base material were analysed using a mobile XRD device in the testing facility in loaded and unloaded condition of the specimens. The results of the local residual stress examinations were in good accordance to the global results [4, 5, 17, 22]. The findings revealed a complex interaction and superposition of the global normal and structural welding stresses and loads and the local restraint stresses [16]. These interactions and several predominant effects are presented in Fig. 11.

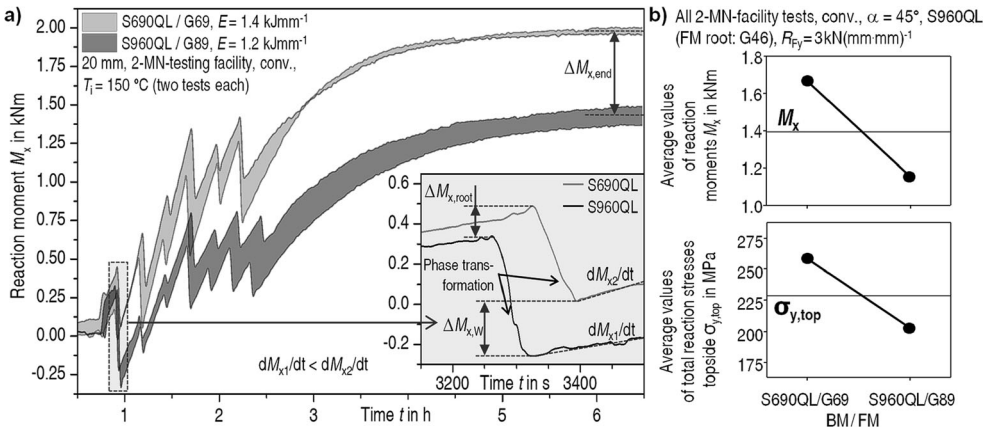

Fig. 10 **a** Reaction moment $M_x(t)$ of restrained welds in the 2-MN-testing facility (restraint intensity $R_{Fy} = 3$ kN(mm mm)$^{-1}$, plate thickness 20 mm) for two different steel grades S960QL/G89 and S690QL/G69, with scatter band; **b** mean values for reaction moments and total reaction stresses at the weld top side vs. steel grade of all weld tests in the 2-MN-testing facility after cooling to RT

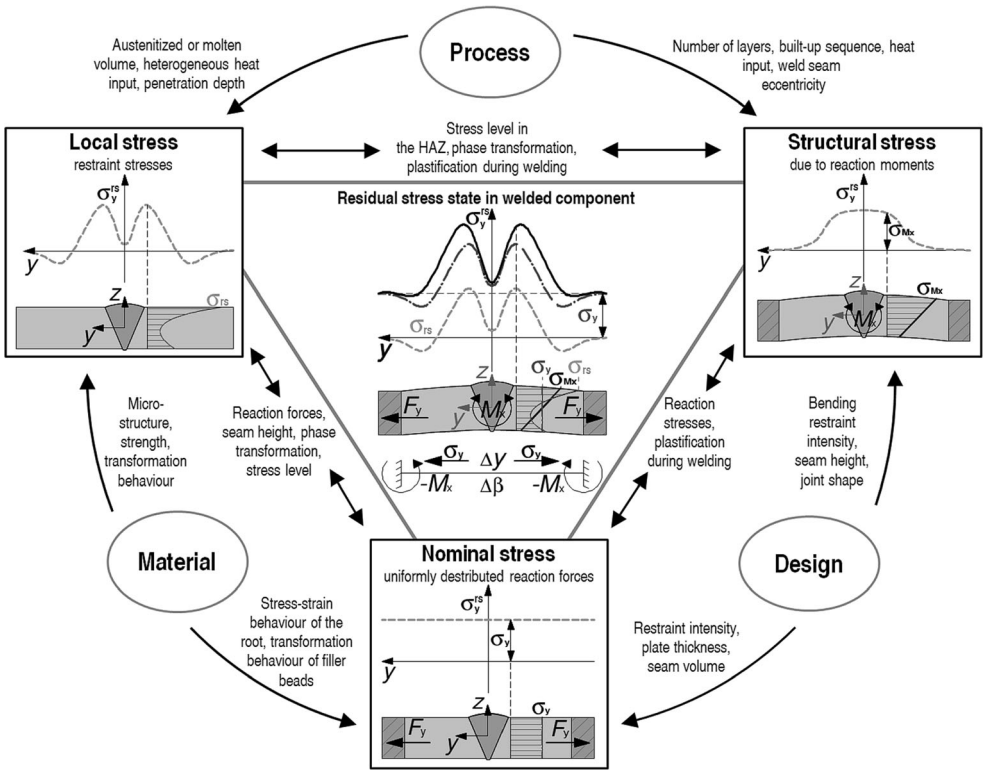

Fig. 11 Derived scheme of the complex interaction of the influencing factors on the welding residual stresses for optimization of the residual stress state in high-strength steel components according to references [4, 15]

On the basis of these experimental findings, the effects and interactions according to the area and type could be analysed, which should help to find an optimised application of filler materials and welding parameters especially in highly restraint welds [4, 16]. In order to assess the global and local welding stresses according to the affected areas and their complex superposition, the metallurgical, process and design induced influences [15] and the interaction of those during and after fabrication of the component welds have to be taken into account.

6 Conclusions

In the present study, the effects and interactions of heat control and steel grade on the formation of multi-axial welding stresses in high-strength steel components were analysed on the basis of the experimental setup of two research projects [13, 14]. Using a special testing machine, in situ analyses of the global reaction forces, moments and stresses in relation to the neutral axis of the actual cross section of the weld was feasible. Multilayer GMA-welding experiments were conducted under defined component-related lateral and angular shrinkage restraint. Thereby, measurements of the welding loads and stresses during and after welding fabrication of high-strength steel components were performed. From the investigations, the following conclusion can be drawn:

(1) It revealed that primarily a low working temperature significantly reduces welding stresses after the completion of the weld. This is due to lower normal reaction stresses and lower reaction moments especially at high restraint conditions after cooling to ambient temperature. The low reaction moments particularly cause reduced bending stresses on the top side of the weld, which are superimposed with the normal reaction stresses and the local residual stresses in the weld.

(2) During fabrication, lower working temperatures lead to increased welding stresses. To prevent crack critical stress levels especially for root welds, adapted fabrication procedures were found.

(3) With the combination of a modified spray arc welding process and a slender seam geometry, an increased load-bearing cross sections of the root welds were realised. With that, both reduced root stresses and, in addition, significantly lower total reaction stresses after completion the weld are achievable.

(4) In high-strength steel constructions, frequently ductile filler materials are applied for root welding. In the analyses, it was observed—for the first time—that in comparison to a matching, an undermatching filler material reduces the reaction moments due to the lower yield strength at temperature of the dominating microstructure, which causes a limitation of the reaction stresses at the top side of the root weld. Lower reaction moment levels due to the root weld

revealed even after completion and cooling of the weld.

(5) The application of higher-strength filler metals for filler beads reduces the reaction moments and stresses due to a beneficial phase transformation behaviour with lower transformation temperatures and a higher percentage of displacive transformation (martensitic).

(6) The local residual stress measurements approved these global results. Based on these experimental findings, the effects and complex interactions according to the area and type (local and global) could be analysed. By taking these effects into account, the welding stresses during and after welding could be optimised. The risk of crack initiation and damages while fabrication and premature failure in service can be reduced and the performance of high-strength steel components as well as the economic application these steel grades can be increased.

Acknowledgements Sincere thanks are given for the support and to the representing companies actively involved in the project board.

Funding information The studies were funded by the AiF-project IGF-Nr. 17267 N (FOSTA P922) and 17978 N (FOSTA P1011).

References

1. Hulka K, Kern A, Schriever U (2005) Application of niobium in quenched and tempered high-strength steels. Mater Sci Forum 500–501:519–526. https://doi.org/10.4028/www.scientific.net/MSF.500-501.519
2. Lu J (2002) Prestress engineering of structural material: a global design approach to the residual stress problem. In: Totten GE, Howes MAH, Inoue T (eds) Handbook of residual stress and deformation of steel. Materials Park, Ohio: ASM International. pp 11–26
3. Eurocode 3: Design of steel structures (EN 1993), 2010
4. Schroepfer D (2017) Adaptierte Wärmeführung zur Optimierung schweißbedingter Beanspruchungen und Eigenschaften höherfester Verbindungen. Dissertation, OVGU Magdeburg, ISBN: 978-3-8440-5406-4
5. Schroepfer D, Flohr K, Kromm A, Kannengiesser T (2017) Multi-axial analyses of welding stresses in high-strength steel welds. In: Mater. Res. Proceedings, Residual Stress. 2016 ICRS-10. Materials research forum, Sydney, pp 205–210
6. Nitschke-Pagel T, Wohlfahrt H (1991) The generation of residual stresses due to joining processes. In: Hauk V, Hougardy H, Macherauch E (eds) Residual stress. - Meas. Calc. Eval. DGM Informationsgesellschaft mbH, ISBN: 3–88355–169-4, pp 121–133
7. Boellinghaus T, Kannengiesser T, Neuhaus M (2005) Effects of the structural restraint intensity on the stress strain build up in butt joints. In: Cerjak H, Bhadeshia HKDH (eds) Math. Model. Weld Phenom. TU Graz, pp 651–669
8. Satoh K (1977) Restraint stresses/ strains v. cold cracking in RRC test of high strength steel. In: Proceedings, Conf. Residual Stress. Welded Constr. Their Eff. The Welding Institute, London, pp 283–289
9. Umekuni A, Masubuchi K (1997) Usefulness of Undermatched weld for high-strength steels. Weld J 76:256–263
10. Schroepfer D, Kannengiesser T (2016) Stress build-up in HSLA steel welds due to material behaviour. J Mater Process Technol 227:49–58. https://doi.org/10.1016/j.jmatprotec.2015.08.003
11. Boellinghaus T, Kannengiesser T (2003) Effect of filler material selection and shrinkage restraint on stress strain build up in component welds. In: Proc. 6th Int. Conf. Trends welding, April. 2002, pine Mt. Georg. USA res. Pine Mt. Georg. USA. ASM international, pp 906–911
12. Satoh K, Terai K, Yamada S et al (1975) Theoretical study on transient restraint stress in multi-pass welding. Transactions Japan Weld Soc 6:42–52
13. Kannengiesser T, Schroepfer D (2014) Fosta P922 - Influence of the weld thermal cycle on residual stress evolution and cold cracking resistance in welded high-strength fine-grained structural steel constructions. Final report (IGF 17267 N), ISBN: 978-3-942541-57-2
14. Kannengiesser T, Schroepfer D (2016) Fosta P1011 - Application of modified spray arc welding to improve welding-specific stressing of high-strength fine-grained structural steel components. Final report (IGF 17978 N), ISBN: 978-3-946885-12-2
15. Karlsson L (1986) Thermal stresses in welding. In: Therm. Stress. I. Sole distributors for the U.S.A. and Canada, Elsevier Science Pub. Co: Amsterdam pp 299–389
16. Schroepfer D, Kromm A, Kannengiesser T (2016) Engineering approach to assess residual stresses in welded components. Weld World 61:91–106. https://doi.org/10.1007/s40194-016-0394-9
17. Schroepfer D, Kromm A, Kannengiesser T (2017) Optimization of welding loads using modified spray arc process. Weld World 61:1077–1087. https://doi.org/10.1007/s40194-017-0484-3
18. Lausch T (2015) Untersuchungen zum Einfluss der Wärmeführung auf die Rissbildung beim Spannungsarmglühen dickwandiger Bauteile aus 13CrMoV9–10. Dissertation, OvGU Magdeburg
19. Rhode M, Kromm A, Kannengiesser T (2012) Residual stresses in multi-layer component welds. In: DebRoy T, Koseki T, David SA, et al (eds) Proc. 9th Int. Conf. Trends Weld. Res. June, 2012, Chicago, USA. ASM International, pp 48–54
20. Kannengiesser T, Lausch T, Kromm A (2011) Effects of heat control on the stress build-up during high-strength steel welding under defined restraint conditions. Weld World 55:58–65. https://doi.org/10.1007/BF03321308
21. Kromm A, Dixneit J, Kannengiesser T (2014) Residual stress engineering by low transformation temperature alloys - state of the art and recent developments. Weld World 58:729–741. https://doi.org/10.1007/s40194-014-0155-6
22. Schroepfer D, Kromm A, Kannengiesser T (2015) Improving welding stresses by filler metal and heat control selection in component-related butt joints of high-strength steel. Weld World 59:455–464. https://doi.org/10.1007/s40194-014-0219-7
23. Bhadeshia HKDH (2004) Developments in martensitic and bainitic steels: role of the shape deformation. Mater Sci Eng A 378:34–39. https://doi.org/10.1016/j.msea.2003.10.328